

# RANS Simulation of Dynamic Trim and Sinkage of a Planing Hull

Parviz Ghadimi\*, Seyed Hamid Mirhosseini, Abbas Dashtimanesh, Mohammad Amini

Department of Marine Technology, Amirkabir University of Technology, Tehran, Iran

\*Corresponding author: pghadimi@aut.ac.ir

Received January 17, 2013; Revised March 22, 2013; Accepted April 22, 2013

**Abstract** In this article, a RANS solver is implemented to model a planing hull motion in calm water. K-E turbulent model is also utilized to capture details around the planing hull and, correspondingly, force acting on the hull. Furthermore, an individual mesh is adopted by combination of structured and unstructured mesh. To verify capability of the considered mesh, steady state solution of a planing hull is investigated and it is observed that numerical settings are adequate for determining planing motion. Finally, a hard chine planing hull is considered and dynamic sinkage and trim are computed. Comparisons of the obtained results with experimental data show a relatively good agreement and it can be concluded that the presented method can be used for practical studies in initial design.

**Keywords:** RANS, planing hull, sinkage, trim, calm water

## 1. Introduction

Seakeeping performance is one of the major concerns of a planing craft. In reality, the seakeeping analysis of the high speed planing hulls is more complex because such vessels exhibit strong non-linearities when operating in a seaway. The studies of the hydrodynamic behavior of planing crafts have been conducted by considerable diversity in approaches. A brief discussion of these modeling schemes is presented in next paragraphs.

There are three primary methods for calculating planing vessel motions, i.e. model experiment (Dong et al., [1]; Yang et al. [2]), 2.5D method, and 3-D CFD method. Aside from experimental investigations (Savitsky [3]; Kaprian and Boyd [4]), most of the theoretical/numerical studies done so far are based on the slender body assumption (Tulin [5], Savander [6], Zhao, Faltinsen and Haslum [7]). The 2.5D method is a kind of slender body theory. 2.5D method provides a means of simplifying a 3D shape into a series of 2-D sections. The problem of a 2-D section with knuckles was analyzed by Arai et al. [8]. The hydrodynamic properties of prismatic planing hulls were investigated using the 2D+T approach by Battistin et al. [9]. Kihara [10] described the computing method for the nonlinear free surface flow including a splash caused by a high-speed vessel and 2.5D method was employed for computation of the wave field of a planing hull in his paper. Lewis et al. [11] used both a RANSE method and the 2-D strip theory to predict high speed craft motion. Sun et al. [12] studied the motion of planing vessels in waves based on the 2D+t theory.

Only few attempts have been made to face the full three-dimensional problem (Lai and Troesch, [13,14]). The recent development of RANS flow solvers makes

them ready for such complicated problem. For 3D CFD method, full Navier-Stokes equation is solved for the flow in a fluid domain. Cao [15] and Wang et al. [16] predicted the resistances of a planing vessel, but the running attitude of planing vessels must be given before the numerical simulation and confirmed through experimentation or the empirical formula. Most literatures report calculation of planing vessel's hydrodynamic performances by the commercial software COMET, which is also believed to be a suitable software to calculate the freedom of the large deformation liquid surface flow, especially in the case of planing vessel. Azcueta et al. [17] used commercial software COMET to simulate a high speed planing vessel. The steady flow computations efficiently create a complete resistance curve in one time - from zero to maximum boat speed - instead of computing only for one speed at a time. The dynamic sinkage and trim are also computed along with the resistance for the whole  $F_n$ -range. Azcueta et al. [18] numerically simulated motions of planing boats in waves based on three different methods. A method by Soding based on an extension of Wagner's theory, and the other two ways (one by Caponnetto, the other by Azcueta) of applying the RANSE solver Comet of this problem. Caponnetto et al. [19] also used COMET software to compute the large deformations of the free surface of typical fast boats. The comparison with the Savitsky method is in general acceptable. The advantage of direct computations lies in the possibility to analyze and compare real hull shapes. Wei et al. [20] used 2-D and 3D methods to compute the slamming force on a planing hull and compare between 3-D and 2-D solutions.

Recently, industry leading design projects in which the authors were involved relied solely on CFD simulations. At Ghadimi's Hydrodynamics Group (GHG), we have forgone traditional towing tank and wind tunnel tests in favor of an exclusively CFD based design philosophy.

Obviously, CFD simulations are cheaper, faster and more reliable than the traditional tests. Simulations are run at full scale which eliminates the inherent error of scaled test results. This relatively new technology can now be successfully taken from the racing environment and applied to the planing hull industry.

In the current article, by implementing a RANS solver, planing craft motion is analyzed and change in dynamic sinkage and trim is studied at high speed regime. It is worth mentioning that the free surface is also simulated by VOF method.

## 2. Governing Equations and Turbulence Modeling

The homogenous multiphase Eulerian fluid approach is adopted in the current study to describe the interface between the water and air, mathematically. Both air and water share the same characteristics (in the free surface) such as velocity, turbulence, etc. The water and air must also be separated by a distinct resolvable interface. The governing equations that need to be solved are the mass continuity equation, which is given as

$$\frac{\partial}{\partial x_i}(\rho u_i) = 0, \quad (1)$$

and the Momentum equations, which are given as

$$\begin{aligned} \frac{\partial}{\partial x_i}(\rho u_i u_j) = & -\frac{\partial p}{\partial x_i} + \frac{\partial}{\partial x_i}(-\rho \bar{u}_i \bar{u}_j) \\ & + \frac{\partial}{\partial x_j} \left[ \mu \left( \frac{\partial u_i}{\partial x_j} + \frac{\partial u_j}{\partial x_i} - \frac{2}{3} \delta_{ij} \frac{\partial u_l}{\partial x_l} \right) \right] \end{aligned} \quad (2)$$

In order to capture the sharp interface of the free surface of the air-water boundary, the volume of fluid method is implemented. A transport equation (i.e. Eq.3) is then solved for the advection of this scalar quantity, using the velocity field obtained from the solution of the Navier-Stokes equations at the last time step.

$$\frac{\partial q}{\partial t} + \vec{\nabla} \cdot (q \vec{u}) = 0 \quad (3)$$

Numerical solution of Eq.3 gives the volume fraction,  $q$ , for each phase (i.e. Air and Water) in all computational cells where  $\sum_{k=1}^2 q_k = 1$ .

Furthermore, a  $k$ - $\varepsilon$  model turbulence model is applied to consider the viscous effects. In this turbulent model,  $k$  is the turbulent kinetic energy and  $\varepsilon$  is the dissipation rate of the turbulent energy. The standard  $k$ - $\varepsilon$  turbulent model in numerical model is presented as follows:

$$\frac{\partial k_i}{\partial x_j} = \frac{\partial}{\partial x_i} \left[ \left( \mu + \frac{\mu_t}{\sigma_k} \right) \frac{\partial k}{\partial x_i} \right] + G_k + G_b - \rho \varepsilon \quad (4)$$

$$\rho u_j \frac{\partial \varepsilon_i}{\partial x_j} = \frac{\partial}{\partial x_i} \left[ \left( \mu + \frac{\mu_t}{\sigma_\varepsilon} \right) \frac{\partial \varepsilon}{\partial x_i} \right] + C_{1\varepsilon} \frac{\varepsilon}{k} (G_k + C_{3\varepsilon} G_b) - C_{2\varepsilon} \rho \frac{\varepsilon^2}{k} \quad (5)$$

where  $G_k$  and  $G_b$  are the generation of turbulent kinetic energy due to the mean velocity gradients and buoyancy. Constant parameters  $\sigma_\varepsilon$ ,  $\sigma_k$ ,  $C_{1\varepsilon}$  and  $C_{2\varepsilon}$  are the model constants and must be determined experimentally. On the other hand,  $\mu_t$  and  $\mu$  are also the turbulent eddy viscosity and the molecular dynamic viscosity, respectively.

## 3. Numerical Modeling and Boundary Conditions

To simulate planing craft motion, inlet-outlet boundary conditions are considered (Figure 1). In this type of simulation, computational cost related to re-gridding and cell deformation are saved. Although viscosity dissipation cannot be modeled accurately, but based on previous studies, considered scheme can lead to reasonable results.

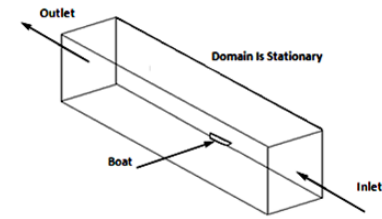


Figure 1. A schematic from considered computational domain

Generally, for calm water simulations, experimental work of Fridsma [21] is considered as a basis of comparison. He performed a series of experiments on planing hull characteristics in calm water motion. He considered a planing hull form which is shown in Figure 2. In the current simulations, planing hull with 30 degrees deadrise angle is considered. Gyration radius is also considered to be 0.25 hull length ( $L$ ). Length to beam ratio ( $L/b$ ) and loading coefficient ( $CA$ ) are equal to 5 and 0.608, successively. Longitudinal position of center of gravity in Fridsma's experiment was 0.6 $L$ . All details about the considered hull is presented in Table 1.

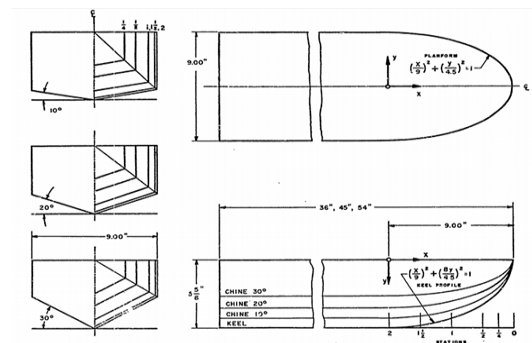


Figure 2. Planing hull considered in Fridsma's experiments

Table 1. Hull characteristics

parameter	Value
$L/b$	5
$b$	0.2286 m
Depth	0.142875 m
Deadrise Angle	30 deg

$c_A = \Delta(lb) / w \times b^3$	0.608
$w$ : (Specified Weight of Water)	62.4 lb / ft <sup>3</sup>
KG	0.294b
LCG from Station Zero	60%L
Pitch Gyradius	25%L

Based on planing hull characteristics, the size of computational domain must be adjusted. Computational domain must be considered to be large enough to remove the wall effects (Figure 3).

In addition to proper selection of computational domain, it is very important to implement appropriate boundary conditions. Based on the considered numerical model, an inlet boundary condition is adopted at the front boundary. Opening boundary condition is also prescribed at aft boundary. No slip condition is another boundary condition which is implemented on the wall and hull. More details about the considered boundary conditions are presented in Figure 4 and Table 2.

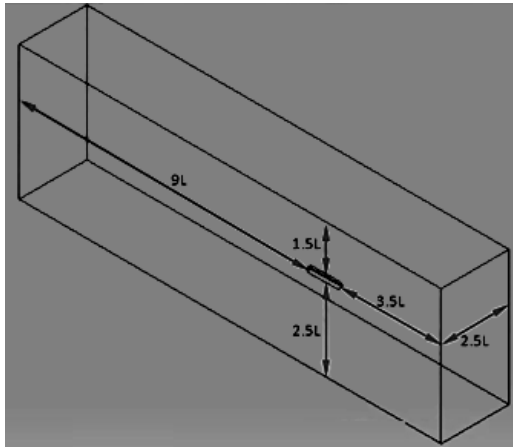


Figure 3. Dimensions of Computational domain

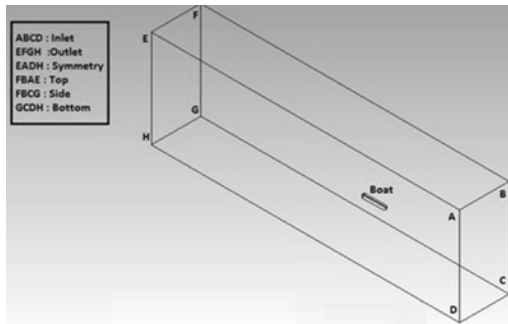


Figure 4. Adopted boundary conditions

Table 2. Details of boundary conditions

Position	Boundary Condition	Type
Inlet	Inlet	Normal Speed
Outlet	Opening	Static Pressure
Top	Opening	Relative Pressure – 0 [Pa]
Bottom	Wall	No Slip
Side	Wall	No Slip
Boat	Wall	No Slip
Symmetry	Symmetry	-----
Rigid Body	Degree Of Freedom : Y Translation and Z Rotation Rigid Body X_Velocity: Zero Speed	

## 4. Mesh Construction and Verification Study

In addition to implementation of numerical model and boundary conditions, a very careful grid refinement is needed in order to obtain an accurate description of the flow field and, correspondingly, of the force acting on the planing hull. The most relevant constraint is the grid resolution needed to capture the sharp gradients taking place in the fore and aft part of the hull. In order to achieve a better understanding of the grid resolution needed for describing such fine details of the flow, computational domain is divided in several sections (as shown in Figure 5). Firstly, two appropriate vertical cuts which are shown by A and B are selected in aft and fore part of the hull. Correspondingly, two horizontal cuts, C and D, are also adopted. Finally, cut FF is considered. Based on the presented segmentation, fine cells can only be adjusted around the hull and consequently, number of computational grids will be decreased, significantly. Moreover, a cut E is also adopted to acquire a smooth VOF solution.

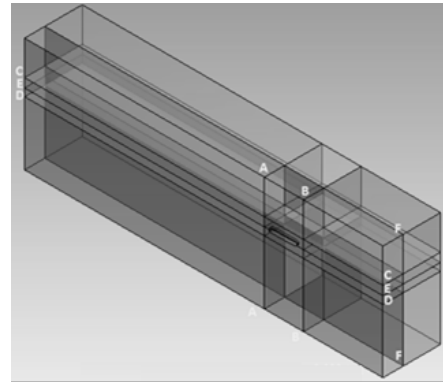


Figure 5. Dividing computational domain for mesh construction

Furthermore, for optimum mesh resolution, it is valuable to use a structured mesh. For this purpose, an unstructured mesh is only adopted around the hull and a structured grid is utilized in other parts of computational domain. Based on our initial studies, mesh size which is presented in Table 3 is adopted for our computations.

Table 3. Mesh size

Size	Region
0.01m	Cells on the hull
0.01m	Unstructured cells
0.01m	cell size in vertical direction near the free surface
0.102m	cell size in the direction of and near the free surface
0.07m	cell size far from the free surface
0.032m	Size of dimension F-F

In continuation of this section, assessment is made on the degree in which the time accurate simulations converge towards steady state for all speeds and to assess the convergence of the steady state solution for the high-speed case as local grid refinement is introduced.

Generally, the computational grid for the high and highest speed cases use roughly 1.2M grid points and performing simulations with finer grids was determined to

be computationally impossible. Estimation of grid uncertainties using multiple solutions with systematically refined grids is not practical and prohibitively expensive for the current problem. Therefore, comparisons with experiments are considered to be mainly qualitative since numerical grid uncertainties are not rigorously estimated. Although the authors are well aware of the importance of conducting verification studies, resource did not allow such studies for the present complex and computationally demanding application.

Moreover, while computational results are discussed in detail later, steady state iterative uncertainties are addressed for all speeds in this section. Computational settings are presented in Table 4 and simulations are conducted at 11 different velocities. Results are compared against experimental data provided by Fridsma [21]. Comparisons show that numerical details which are adopted in RANS simulations are completely in good agreement with the physical characteristics of the problem, as shown in Figure 6. In fact, the obtained resistance from RANS solutions is in excellent agreement with the experimental data. Therefore, it can be concluded that considered numerical setting may be suitable for future unsteady solutions.

Table 4. Computational setting for steady state solutions

Parameter	Setting
Analysis Type	Steady
Multiphase Model	Homogeneous
Turbulence Model	$k-\epsilon$
Convergence Criteria	RMS 1E-4
Spatial Discretization Scheme	High Order
Time Discretization Scheme	2 <sup>nd</sup> Order Backward Euler
Run Mode	Parallel On Corei7

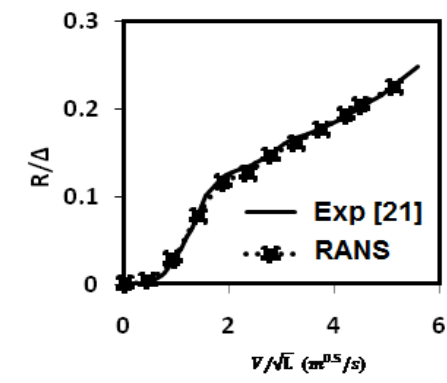


Figure 6. Steady state solution of hull resistance

## 5. Results and Discussions

In the previous sections, details of the presented study including governing equations, numerical modeling, boundary conditions and mesh construction are thoroughly discussed. Therefore, it is now appropriate to present numerical solutions. Based on the previous sections, setting which is proposed in Table 5 is adopted.

Table 5. Computational setting for transient solutions

Parameter	Setting
Analysis Type	Transient

Time Step	0.01[s]
Multiphase Model	Homogeneous
Turbulence Model	$k-\epsilon$
Convergence Criteria	RMS 1E-4
Spatial Discretization Scheme	High Order
Time Discretization Scheme	2 <sup>nd</sup> Order Backward Euler
Rigid Body Motion	Y Translation and Z Rotation
Initial Condition	U Velocity = -Inlet Velocity [m/s] V Velocity=0 [m/s] W Velocity=0 [m/s] Pressure = Static Pressure
Run Mode	Parallel On Corei7

Nine different velocities are considered and simulations are performed until heave and pitch become steady. In Figure 7, rise of planing hull is presented and compared against experimental data. Generally, simulation results can be divided into two main parts:  $V/\sqrt{L} < 2.79$  and  $V/\sqrt{L} > 2.79$ . In the first regime, reasonable results are achieved. However, in the second regime, obtained results are not desirable. Therefore, it can be concluded that the presented solution must be improved for a very high speed case.

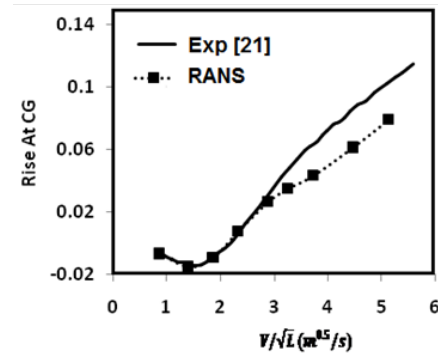


Figure 7. Rise of planing hull at various velocities

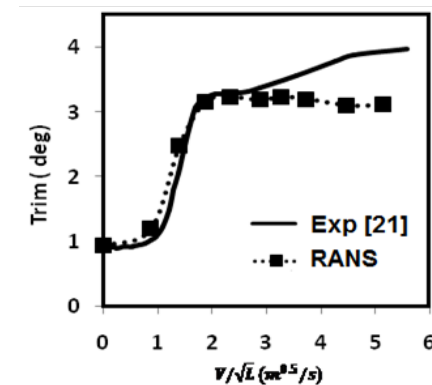


Figure 8. Comparison of the obtained trim against experimental results

Furthermore, based on Figure 7 and Figure 8 it is observed that at  $1.4 < V/\sqrt{L} < 2.79$ , transient condition exists and planing hull passes the planing criteria. This means that numerical solution can recognize planing behavior. However, accuracy of solution decreases after transient situation. Mentioned inaccuracy is also visible in prediction of resistance as well (as shown in Figure 9). It is clear that resistance is a function of rise and trim, because previous inconsistencies in rise and trim are also observed in the results related to the resistance. Authors believe that the observed inconsistencies are due to mesh

dependencies, rigid body motion and nonlinearity existing in the problem. Average error of the presented solution is presented in Table 6.

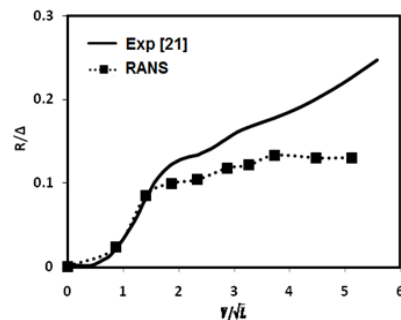


Figure 9. Comparison of Planing hull resistance against the experimental data

Table 6. Average error

$V / \sqrt{L}$	Mean Error %
Heave Motion	16.07%
Pitch Motion	11.13%
Resistance	44.35%

## 6. Conclusions

In the current article, a RANS solver is implemented to solve highly nonlinear problem of planing craft motion in calm water. In this context, Navier-Stokes equations are considered as governing equations and a k-E turbulence model is adopted. Furthermore, an individual mesh is constructed and it is shown that presented numerical schemes are suitable for planing motion simulations.

Based on verification study, a general setting is found for simulations which are conducted at nine different velocities. To validate RANS solutions, the obtained results are compared against experimental data and it is observed that RANS solutions are in relatively good agreement with the experimental results and can be used in initial design of planing hulls. In fact, after transient condition, RANS solver cannot capture all physics that occur in flow field. Therefore, it is necessary to improve simulations accuracy in future studies. Moreover, a detailed mesh convergence studies should be investigated with more powerful computers.

## References

- [1] Wencai, D. Xiangbing, H. Zhihua, L., "Experimental determination of roll damping of deep-Vee planing craft". *Journal of Naval University of Engineering*, 16(4), 26-29, 2004.
- [2] Songlin, Y., Lei, G., "Experimental study on resistance performance of an 11.8 meter gliding-hydrofoil craft". *Journal of Jiangsu University of Science and Technology (Natural Science Edition)*, 22(2), 6-10, 2008.
- [3] Savitsky, D., "Hydrodynamic design of planing hulls," *Mar. Tch.*, Vol. 1, p.71, 1964.
- [4] Kaprian, W.J., and Boyd, G.M. Jr., "Hydrodynamic pressure distribution obtained during a planing investigation of vive related planing surface", *Tech. Report, TN 3477, NACA*, 1955.
- [5] Tulin, M.P., "The theory of slender surfaces planing at high speed", *Schiffstechnik*, Vol. 4, p.125, 1956.
- [6] Savander, B.R., "Planing hull hydrodynamics," *PhD thesis, Dept. NAME, Univ. Michigan, Ann Arbor (MI), US*, 1997.
- [7] Zhao, R., Faltinsen, O. and Haslum, H., "A simplified nonlinear analysis of a high speed planing craft in calm water", *Proc. FAST 97 Conf., Sydney*, p.431, 1997.
- [8] Arai M, Cheng LL, Inoue Y., "A computing method for the analysis of water impact of arbitrary shaped bodies", *Journal of the Society of Naval Architects of Japan*, 176, 233-239, 1994.
- [9] Battistin, D, Iafrazi, A., "A numerical model for hydrodynamic of planing surfaces". *Proc.7th Int. Conf. Fast Sea Transportation FAST2003, Nanjing*, 33-38, 2003.
- [10] Kihara, H. "A computing method for the flow analysis around a prismatic planing-hull. 7th international conference on high performance marine vehicles". *Yokosuka, Australian*, 262-272, 2006.
- [11] Lewis, S.G., Hudson, D.A., Turnock, S.R., Blake, J.I.R., Sheno, R.A. Predicting motions of high speed RIBs: A comparison of non-linear strip theory with experiments. *Proceedings of the 5th International Conference on High Performance Marine Vehicles (HIPER'06), Launceston, Australia*, 210-224, 2006.
- [12] Sun, H., Faltinsen, O.M., "Numerical study of planing vessels in waves". *9th International Conference on Hydrodynamics, Shanghai*, 451-458, 2010.
- [13] Lai, C., and Troesch, A.W., "Modeling issues related to the hydrodynamics of three-dimensional steady planing," *J. Ship Res.*, Vol. 39, p.1, 1995.
- [14] Lai, C., and Troesch, A.W., "A vortex lattice method for high speed planing," *Int. J. Num. Meth. Fluids*, Vol. 22, p.495, 1996.
- [15] Cao, H., "The Computation and research on resistance of planing craft based on the software FLUENT". *PhD thesis. Harbin Engineering University, Harbin*, 44-53. Dong Wencai, 2008.
- [16] Wang, Z., Niu, J., Qin, Z., Pang, Y., "The computation resistance of planing craft based on the CFD techniques". *14th Conference on China Ocean Engineering, Hohhot*, 309-315, 2009.
- [17] Azcueta, R., "Steady and unsteady RANSE simulations for planing RAFTS". *7th Conference on Fast Sea Transportation, FAST'03, Abano Terme, Italy*, 2003.
- [18] Azcueta, R., "Caponnetto, M., Soding, H., "Motion simulations for planing boats in waves". *Ship Technology Research*, 4, 182-198, 2003.
- [19] Caponnetto, M., "Practical CFD simulations for planing hulls". *Proc. of Second International Euro Conference on High Performance Marine Vehicles, Hamburg*, 128-138, 2001.
- [20] Qiu, W., Yang, Q., "Peng Heather. Slamming force on a planing hull: Comparison between 3D and 2D solutions". *Proceedings of the 18th International Offshore and Polar Engineering Conference, Vancouver, Canada*, 2008.
- [21] Fridsma, G., "A Systematic Study of the Rough-Water Performance of Planning Boats". Report 1275, Davidson Laboratory, Stevens Institute of Technology, Hoboken, New Jersey, 1969.